Supplementary Information

Composition-dependent hydrogen oxidation activity of Pt-Cu nanoparticles prepared using boron-rich nanosheets

Bhagyashri Gaykwad,[a,b] Donald A. Robinson,[a] Nicholas Humphrey,[a] Samuel F. Wenzel,[c] Carly Hui,[a] Natalia McCoy,[a] Farid El Gabaly,[a] Joshua D. Sugar,[a] Matthew D. Witman,[a] Kabeer Jasuja,[b] Hang Ren,[c*] Vitalie Stavila[a*]*

[a] Sandia National Laboratories, Livermore, CA 94551, United States

[b] Indian Institute of Technology, Gandhinagar, Gujarat 382055, India

[c] Department of Chemistry, Allen J. Bard Center for Electrochemistry, Texas Materials Institute, The University of Texas at Austin, Austin, TX 78712, United States

Experimental Section

1. Electrocatalyst Synthesis

Synthesis of MgB_2-derived nanosheets

The boron nanosheets (BNS) were synthesized according to a recipe mentioned in an earlier report.[1,2] Briefly, 1.15 g magnesium diboride (MgB_2) powder was mixed with 250 mL of 0.1M disodium EDTA solution. The pH of the solution was maintained between 8 and 9 for optimal Mg-complexation using 1M NaOH. This solution was magnetically stirred at 300 rpm for one hour, with the temperature maintained at ≈22 °C. The solution was left to settle for a day, after which the clear top part was recovered by two rounds of centrifugation at 3000 rpm for 30 min. The final supernatant was dialyzed against DI water (to remove residual salts and ionic species) using cellulosic dialysis sacks (22 mm diameter, 3.5 kDa molecular weight cut off, Sigma) for ~30 hours to obtain a transparent colloidal dispersion of nanosheets.

Synthesis of bimetallic (PtCu) decorated hybrid structures using MgB_2-derived nanosheets

Solutions containing chloroplatinic acid hexahydrate (Sigma Aldrich) and copper (II) nitrate trihydrate (Sigma Aldrich) were combined in different mole ratios (Pt: Cu = 0:1, 0.1:0.9, 0.25:0.75, 0.5:0.5, 0.75:0.25, 0.9:0.1, 1:0) to prepare a 10 mM mixed metal salt solution (Table S1). For each synthesis, 20 mL of the mixed metal solution was stirred at 500 rpm for 10 min. Next, 100 mL of an aqueous dispersion of dialyzed BNS (1.66 mg/mL) was added and the solution was stirred for one hour at ambient conditions (temperature ~21 °C). Here, with the progression of time, we observed different degrees of colour change with varying Pt and Cu salt ratios. After 24 hr, Pt/BNS and Pt:Cu/BNS precipitates were collected from suspension by centrifugation (8000 rpm), and washed with water by resuspending and collecting by centrifuge two more times, followed by one resuspension in isopropanol and collection by centrifugation. The fine dispersion of Cu/BNS resulting from the Pt-free synthesis with only copper nitrate and boron nanosheets was purified by dialysis using SnakeSkin™ membrane tubes (3.5 kDa cutoff). All products were dried under vacuum at 60 °C.

Table S1: *Quantitative proportions of platinum and copper precursors used during the synthesis of PtCu/BNS hybrid nanostructures before addition of BNS dispersion.*

S.no	Pt:Cu mol ratio	$[PtCl_6^{2-}]$ (mM)	$[Cu^{2+}]$ (mM)
1	0:1	0	10
2	1:9	1	9
3	1:3	2.5	7.5
4	1:1	5	5
5	3:1	7.5	2.5
6	9:1	9	1
7	1:0	10	0

2. Characterization

Powder X-ray diffraction (PXRD) patterns of powder samples were measured by Oxford Diffraction Supernova in the 2θ range of 5° to 90°. Rietveld refinements were performed using the software package HighScore Plus.

X-ray photoelectron spectroscopy (XPS) measurements were performed using an Omicron Model DAR400 X-ray source equipped with an Al Kα source, which emits photons at an energy of 1486.6 eV. The depth sensitivity of XPS is about 5 nm from the surface. Photoelectrons were detected using a Physical Electronics Model 10-360 analyzer. Binding energies were calibrated to position the adventitious carbon C1s peak at 284.8 eV.

The metal contents of the catalysts were analyzed by inductively coupled plasma optical emission spectroscopy (PerkinElmer Avio 200 instrument) located at the Indian Institute of Technology Gandhinagar (IITGN).

The morphological structure and elemental composition of the samples were captured by a transmission electron microscope (TEM) (Thermo Fisher Titan Themis Z), operated at an accelerating voltage of 300 kV, located at Sandia National Laboratories (SNL). Annular Dark Field Scanning Transmission Electron Microscopy (ADF-STEM) was performed with a probe-corrected JEOL NEOARM operated at an accelerating voltage of 200 kV, located at the Texas Materials Institute (TMI) at the University of Texas at Austin. Image processing & Electron Energy Loss Spectroscopy (EELS) analyses were accomplished using Gatan DigitalMicrograph Software.

3. Electrochemical measurements

Catalyst inks were prepared by suspending the catalyst powders in a solution containing 49.5% v/v water, 49.5% v/v ethanol, and 1% v/v of Nafion™ D520C alcohol-based dispersion (5 % wt polymer, Ion Power). An ink containing the reference Pt/C catalyst (20 wt% Pt, Sigma Aldrich) was prepared in a similar manner. A 2.5 μL volume of the ink was dropcast on a glassy carbon rotating disk electrode (RDE, 3 mm diameter) and allowed to dry.

Electrochemical measurements were recorded using a Biologic potentiostat (SP-200) and electrode rotator (Autolab RDE, Metrohm). All experiments were performed at 294 K in a Teflon cell containing 0.1 M KOH. Au wire was used as the counter electrode. Potentials were recorded vs a Hg/HgO reference electrode (0.1 M KOH filling solution) and converted to potential vs RHE based on the potential at zero current for a Pt RDE under 1 atm H_2.

Prior to voltametric measurements, the open circuit potential of the catalyst-modified films in the electrolyte was monitored until reaching a steady state. Uncompensated solution resistance was measured from the ac impedance at 100 kHz, taking the real part of the impedance as the cell resistance, giving a solution resistance of 66 Ω. Pt ECSA measurements were performed by cyclic voltammetry in Ar-purged electrolyte. The charge associated with the anodic desorption of underpotential-adsorbed hydrogen on Pt was used to determine the Pt-specific electrochemically active surface area (ECSA), converting charge to surface area using conversion factors of 210 μC/cm^2 and 176 μC/cm^2 for the nanoparticle catalysts and polycrystalline platinum disk, respectively.[3] HOR voltammetric traces were processed by correcting the measured potential to account for solution resistance. Measured HOR currents (j_m) at varied rotation rates (ω) were analysed using the Koutecky-Levich equation (eq 1), to obtain the Levich constant, B, from the slope of j_m^{-1} plotted versus $\omega^{-1/2}$.

$$\frac{1}{j_m} = \frac{1}{j_k} + \frac{1}{B\omega^{1/2}} \quad (1)$$

The measured currents in the low overpotential region (0 to 20 mV) were then converted to the kinetically limit current, j_k, which was normalized by Pt ECSA for Pt-specific activity or the loading Pt mass for Pt-mass activity. Apparent exchange current density, j_0^{app}, was estimated from the linear relationship of j_k to overpotential, η, in the micropolarization regime.[4, 5]

$$\frac{j_k}{\eta} = \frac{F}{RT} j_0^{app} \quad (2)$$

4. Computational details

Simulation cells of Pt and Cu in the FCC phase with 32 atoms were converged until forces less than 10^{-3} eV/Å were achieve with VASP. The Pt and Cu electrons are described with $5p^6\ 5d^9\ 6s^1$ and $3p^6\ 3d^{10}\ 4s^1$ respectively with an energy cutoff of 500 eV and treated with PBE. The spin polarized calculations are carried out with Methfessel-Paxton of the order 1, a smearing of 0.2 eV, for atomic relaxations and Tetrahedron method with Blöchl corrections without smearing for electronic calculations to determine the d-band energy. The number of bands is 288 to account for occupied and unoccupied *s*, *p*, and *d* bands of the transition metals. The lattice was sampled with a 4x4x4 Γ-centered k-point mesh. Following atomic relaxation of the Pt FCC lattice, Pt atoms are randomly selected to substitute for Cu atoms, and the lattice is scaled according to Vegard's Law with the use of the Atomic Simulation Environment[6]. Ten samples are generated for each composition ranging from 1:31 Pt:Cu to 31:1 Pt:Cu, and the DScribe package[7] with periodic enabled Smooth Overlap of Atomic Positions (SOAP) is utilized to determine and compare the chemical environments of the generated structures. The cutoff for local region is 5 Å, and the number of radial basis functions and maximum degree of spherical harmonics are 2 for SOAP. REMatch kernal in the DScribe package identified any structures that are already sampled[8] and another structure is generated to avoid sampling multiple times. The VASPkit package[9] is used to evaluate the d-band[10, 11] of the bulk metal alloys, and the d-band is averaged over all structures at the current composition. The d-band following relaxation of the cell and atoms was determined to be qualitatively similar to d-band calculations on unoptimized alloy structures.

Hydrogen binding was calculated on the 111 surface of a 4 layer slab with 64 metal atoms. The surface was constructed with the ASE package from the bulk lattice determined form Vegards Law, with repeating of the surfaces by 2 (16 atoms/layer) so the hydrogen atom does not self interact, and a vacuum of 15 Å added to both sides to prevent self interactions. Atoms were randomly selected to replace Pt with Cu for every 10% composition. The slab atoms are relaxed to a 0.1 eV/Å threshold with the universally trained MACE potential. Hydrogen atoms are bound to all ontop, bridged, and hollow type sites for a total of 1056 hydrogen binding energies. Large sampling must be done because there are many different types of local atomic environments on the surface of the Cu-Pt alloy, which is why we opted for use of the MACE potential instead of DFT. Table S2 shows the averaged results.

***Table S2**: Average hydrogen binding energies for FCC Cu-Pt alloy 111 surfaces*

Precent of Cu (%)	Ontop BE (eV)	STD	Bridge BE (eV)	STD	Hollow BE (eV)	STD	All average (eV)	STD
0%	-0.67	0.00	-0.65	0.00	-0.60	0.04	-0.64	0.04
10%	-0.56	0.25	-0.70	0.05	-0.67	0.12	-0.67	0.14
20%	-0.58	0.11	-0.62	0.10	-0.64	0.09	-0.62	0.10
30%	-0.42	0.36	-0.56	0.06	-0.59	0.05	-0.55	0.16
40%	-0.37	0.32	-0.54	0.15	-0.57	0.13	-0.53	0.20
50%	-0.34	0.34	-0.59	0.17	-0.55	0.18	-0.54	0.23
60%	-0.41	0.18	-0.51	0.16	-0.48	0.17	-0.49	0.17
70%	-0.37	0.15	-0.43	0.11	-0.42	0.15	-0.42	0.14
80%	-0.29	0.11	-0.34	0.14	-0.34	0.14	-0.33	0.14
90%	0.03	0.30	-0.23	0.09	-0.25	0.07	-0.19	0.17
100%	0.37	0.00	-0.08	0.00	-0.21	0.01	-0.05	0.20
Number of sites	16		48		32		96	

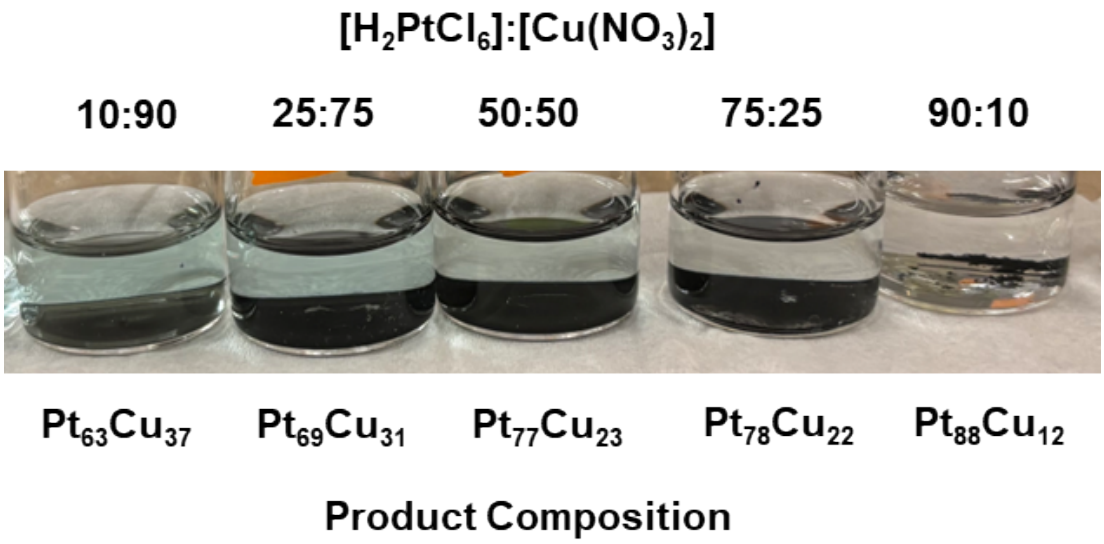

Figure S1: Images of synthesis reaction mixtures after allowing precipitated PtCu nanoparticles to settle, showing blue coloration of supernatant attributed to unreacted Cu^{2+} for samples synthesized with $[H_2PtCl_6]$:$[Cu(NO_3)_2]$ molar ratios of 10:90, 25:75, and 50:50.

***Table S3**: Ratios of B and Mg to metal (M) and B/Mg obtained from ICP-OES*

Sample	B/M	Mg/M	B/Mg
Pt_0Cu_{100}/BNS	14	3.9	3.7
$Pt_{63}Cu_{37}$/BNS	1.4	0.11	13
$Pt_{69}Cu_{31}$/BNS	0.34	0.04	9.4
$Pt_{77}Cu_{23}$/BNS	0.39	0.05	7.7
$Pt_{78}Cu_{22}$/BNS	0.17	0.02	11
$Pt_{88}Cu_{12}$/BNS	0.11	0.01	7.8
$Pt_{100}Cu_0$/BNS	0.05	0.01	5.2

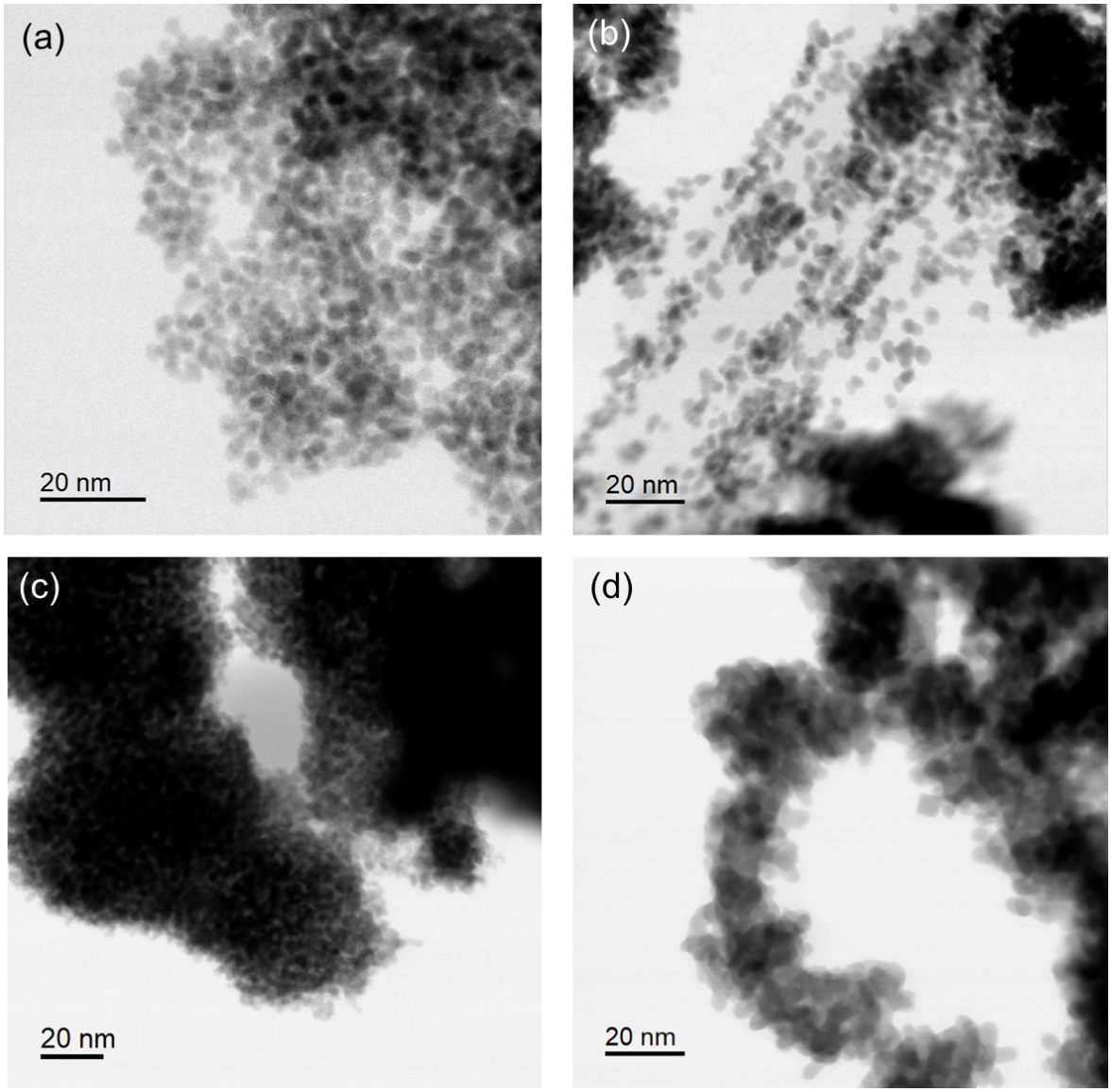

Figure S2: Bright field STEM images of (a) $Pt_{63}Cu_{37}$/BNS, (b) $Pt_{69}Cu_{31}$/BNS, (c) $Pt_{77}Cu_{23}$/BNS and (d) Pt/BNS.

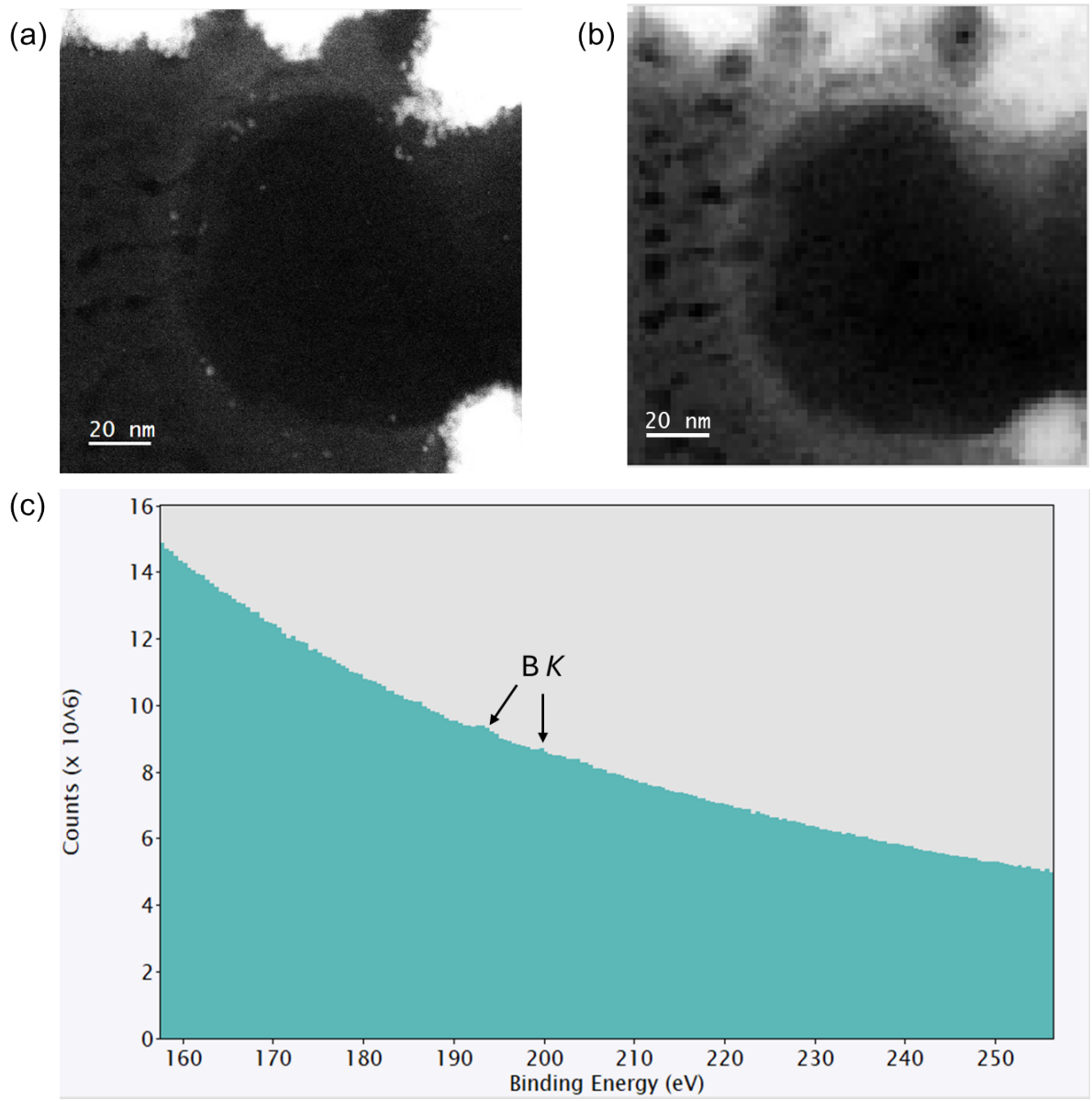

Figure S3: (a) ADF STEM image of $Pt_{77}Cu_{23}$/BNS, (b) corresponding EELS map, and (c) corresponding EELS spectrum with labelled B K-edge energy peaks.

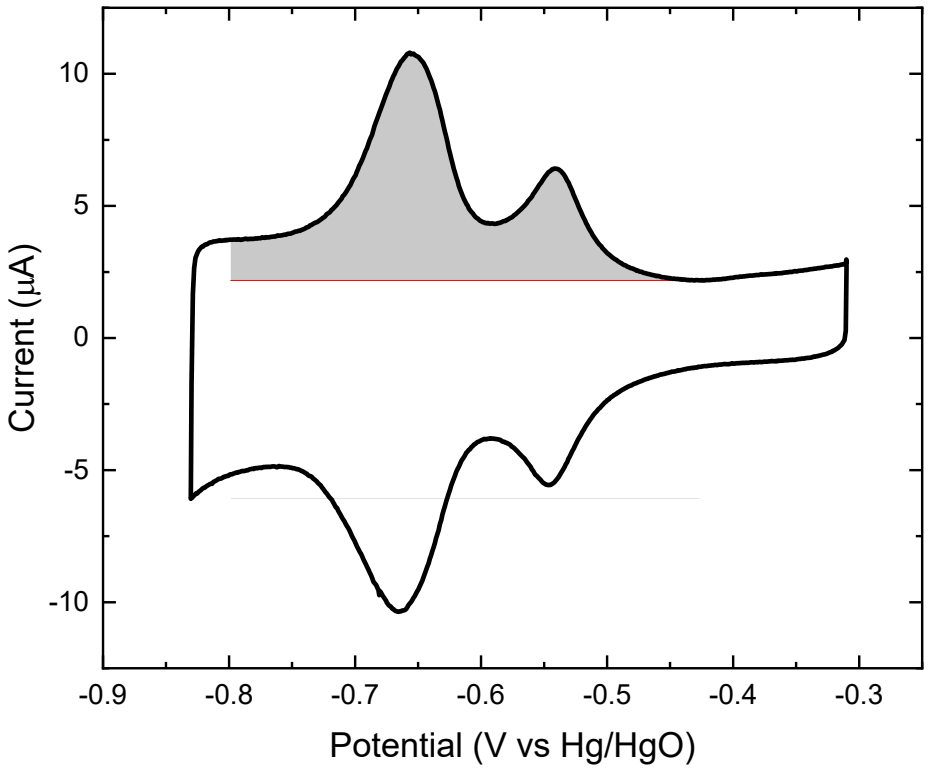

Figure S4: Example cyclic voltammogram of Pt-H_{UPD} adsorption/desorption region of $Pt_{63}Cu_{37}$/BNS on glassy carbon RDE in Ar-purged 0.1 M KOH, 10 mV/s. Shaded region indicates the area for integration to estimate H desorption charge used for determining the ECSA value assuming 210 μC/cm^2_{Pt}.

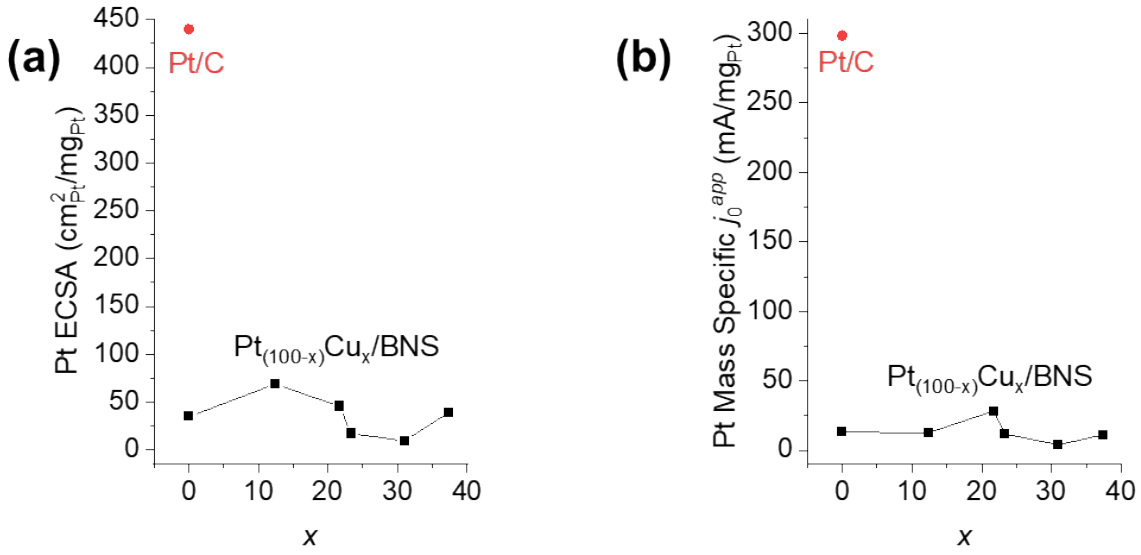

Figure S5: (a) Pt-specific ECSA values and (b) Pt mass specific exchange currents obtained for Pt/C and $Pt_{(100-x)}Cu_x$/BNS catalysts.

***Table S4**: Catalyst mass loading for HOR experiments**

Sample	Pt wt%	Total Loading ($\mu g/cm^2$)	Pt Loading ($\mu g_{Pt}/cm^2$)
Pt_0Cu_{100}/BNS	0	248	0
$Pt_{63}Cu_{37}$/BNS	74.6	248	185
$Pt_{69}Cu_{31}$/BNS	84.6	248	210
$Pt_{77}Cu_{23}$/BNS	88.1	248	218
$Pt_{78}Cu_{22}$/BNS	90.5	248	224
$Pt_{88}Cu_{12}$/BNS	94.8	248	235
$Pt_{100}Cu_0$/BNS	99.6	124	123
Pt/C	20	35	7.1

*Mass loadings were chosen based on the necessary amount of catalyst to achieve a similar transport-limited HOR current compared to the Pt disk rotating disk electrode at 1600 rpm. All electrode geometric areas were 0.071 cm^2 (3.0 mm diameter).

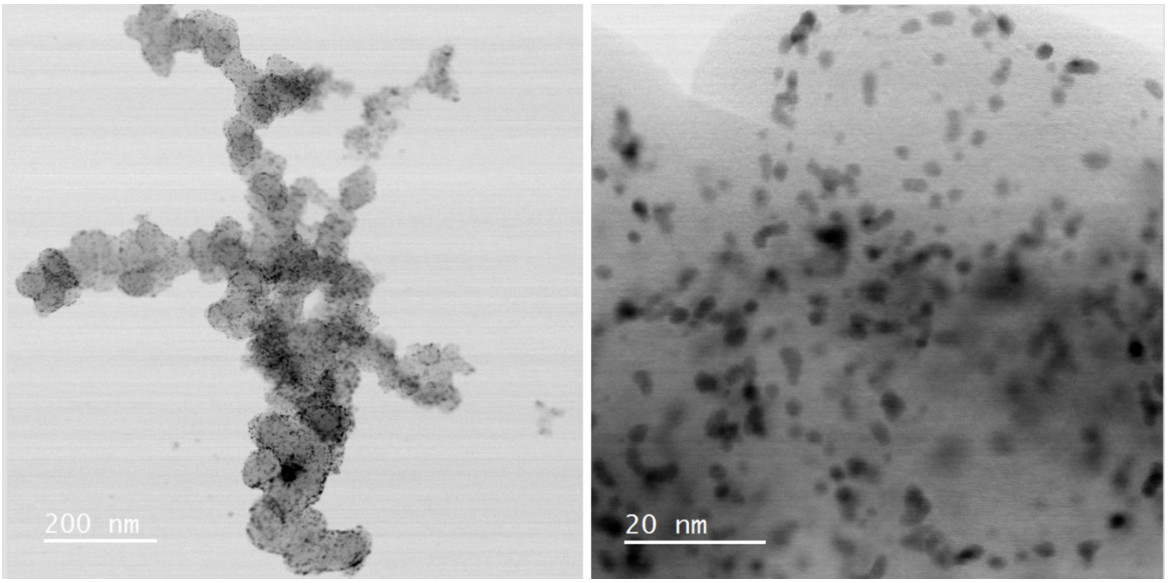

Figure S6: Bright field STEM images of the Pt/C reference catalyst.

5. References:

1. A. L. James and K. Jasuja, *RSC Adv.*, 2017, **7**, 1905-1914.
2. R. Saraswat, A. L. James and K. Jasuja, *Adv. App. Ceram.*, 2019, **118**, 209-216.
3. C. Wei, R. R. Rao, J. Peng, B. Huang, I. E. L. Stephens, M. Risch, Z. J. Xu and Y. Shao-Horn, *Adv. Mater.*, 2019, **31**, 1806296.
4. A. J. Bard, L. R. Faulkner and H. S. White, *Electrochemical methods: fundamentals and applications*, John Wiley & Sons, 2022.
5. A. R. Kucernak and C. Zalitis, *J. Phys. Chem. C*, 2016, **120**, 10721-10745.
6. A. Hjorth Larsen, J. Jørgen Mortensen, J. Blomqvist, I. E. Castelli, R. Christensen, M. Dułak, J. Friis, M. N. Groves, B. Hammer, C. Hargus, E. D. Hermes, P. C. Jennings, P. Bjerre Jensen, J. Kermode, J. R. Kitchin, E. Leonhard Kolsbjerg, J. Kubal, K. Kaasbjerg, S. Lysgaard, J. Bergmann Maronsson, T. Maxson, T. Olsen, L. Pastewka, A. Peterson, C. Rostgaard, J. Schiøtz, O. Schütt, M. Strange, K. S. Thygesen, T. Vegge, L. Vilhelmsen, M. Walter, Z. Zeng and K. W. Jacobsen, *J. Phys.: Condens. Matter*, 2017, **29**, 273002.
7. J. Laakso, L. Himanen, H. Homm, E. V. Morooka, M. O. J. Jäger, M. Todorović and P. Rinke, *J. Chem.Phys.*, 2023, **158**, 234802.
8. S. De, A. P. Bartók, G. Csányi and M. Ceriotti, *Phys. Chem. Chem. Phys.*, 2016, **18**, 13754-13769.
9. V. Wang, N. Xu, J.-C. Liu, G. Tang and W.-T. Geng, *Comput. Phys. Commun.*, 2021, **267**, 108033.
10. S. Bhattacharjee, U. V. Waghmare and S.-C. Lee, *Sci. Rep.*, 2016, **6**, 35916.
11. B. Hammer and J. K. Nørskov, *Surf. Sci.*, 1995, **343**, 211-220.